Journal of Applied Polymer Science

# Assessment of cell proliferation in knitting scaffolds with respect to pore-size heterogeneity, surface wettability, and surface roughness

A Ra Jo,[1] Myoung Wha Hong,[2] Yong Sang Cho,[1] Ki Myoung Song,[1] Jun Hee Lee,[3] Dongwoo Sohn,[4] Young-Yul Kim,[2] Young-Sam Cho[1]

[1]Division of Mechanical and Automotive Engineering, College of Engineering, Wonkwang University, 460 Iksandae-ro, Iksan, Jeonbuk 570-749, Republic of Korea

[2]Department of Orthopedics, Deajeon St. Mary's Hospital, Catholic University of Korea, 64, Daeheung-ro, Jung-gu, Daejeon 301-723, Republic of Korea

[3]Department of Nature-Inspired Nano Convergence System, Nano Convergence and Manufacturing Systems Research Division, Korea Institute of Machinery and Materials (KIMM), 156, Gajeongbuk-Ro, Yuseong-Gu, Daejeon 305-343, Republic of Korea

[4]Division of Mechanical Engineering, College of Engineering, Korea Maritime and Ocean University, 727 Taejong-ro, Yeongdo-gu Busan 606-791, Republic of Korea

Correspondence to: Y.-Y. Kim (E-mail: kimtwins72@catholic.ac.kr) and Y.-S. Cho (E-mail: youngsamcho@wku.ac.kr)

**ABSTRACT:** In this study, various types of poly(ε-caprolactone) (PCL) knitting scaffolds were fabricated and analyzed to assess the cell-culturing characteristics of knitting scaffolds with respect to pore-size heterogeneity, surface wettability, and surface roughness. First, control knitting scaffolds were fabricated using 150-μm-diameter PCL monofilaments. Using chloroform and NaOH, PCL knitting scaffolds with varying roughness, pore-size heterogeneity, and surface wettability were fabricated. Cell-culture assessments were performed on these six types of PCL knitting scaffolds. Saos-2 cells were used for cell assessments and cultured for 14 days on each scaffold. Consequently, heterogeneous pore-size distribution and high surface wettability were found to enhance cell proliferation in knitting scaffolds. In addition, for highly hydrophobic knitting scaffolds exhibiting water contact angles greater than 110 degrees, smaller surface roughness was found to enhance cell proliferation. According to this study, in the case of knitting scaffold, NaOH-treated knitting scaffold, without any control for the pore-size homogenization, could be a candidate as the optimal knitting scaffold.
 J. Appl. Polym. Sci. **2015**, *132*, 42566.

**KEYWORDS:** biomedical applications; biomaterials; properties and characterization

Received 25 February 2015; accepted 1 June 2015
**DOI: 10.1002/app.42566**

## INTRODUCTION

Tissue engineering for the regeneration of damaged or malfunctioning organs is unlike conventional medical treatments for restoring damaged human organs and tissues.[1,2] In tissue engineering, to restore damaged tissues, a three-dimensional porous structure called a scaffold is needed for cell proliferation.[3–5] Scaffolds should have structures that facilitate the supply of nutrients and oxygen, as well as waste discharge.[6,7] In general, this requirement of scaffolds has been accomplished via porosity and interconnected pores.[8–10] Moreover, the scaffold should be biocompatible, biodegradable, and appropriate mechanical property. To satisfy requirements of scaffold, several studies used biocompatible and biodegradable synthetic polymer such as poly(L)lactide (PLA),[11] poly(L-lactic acid) (PLLA),[12,13] poly (lactic-co-glycolic acid) (PLGA),[14,15] poly(ε-caprolactone) (PCL).[16–18] PCL which is one of synthetic polymer has good processibility by low melting temperature, cost effectiveness, and mechanical property.[10,17,18] Therefore, to fabricate knitting scaffolds, PCL was used.

Scaffolds should have high surface areas for cell adhesion and proliferation.[19–22] To address the surface area issue, we proposed a knitting technique in a previous study using biocompatible and biodegradable polymer monofilament.[23] Knitting scaffolds contain interconnected pores intrinsically. Furthermore, if small diameter monofilaments are used, scaffold surface areas are larger than solid freeform fabrication (SFF) scaffolds which are widely used in scaffold fabrication generated using a deposition system.[24–27] Knitting scaffolds have intrinsic characteristics such as non-homogeneous pore-sizes and a smooth surface. Because knitting scaffolds were first proposed by our group in our previous study, the characteristics of knitting scaffolds are not yet clearly understood. Therefore, in this study, several parametric

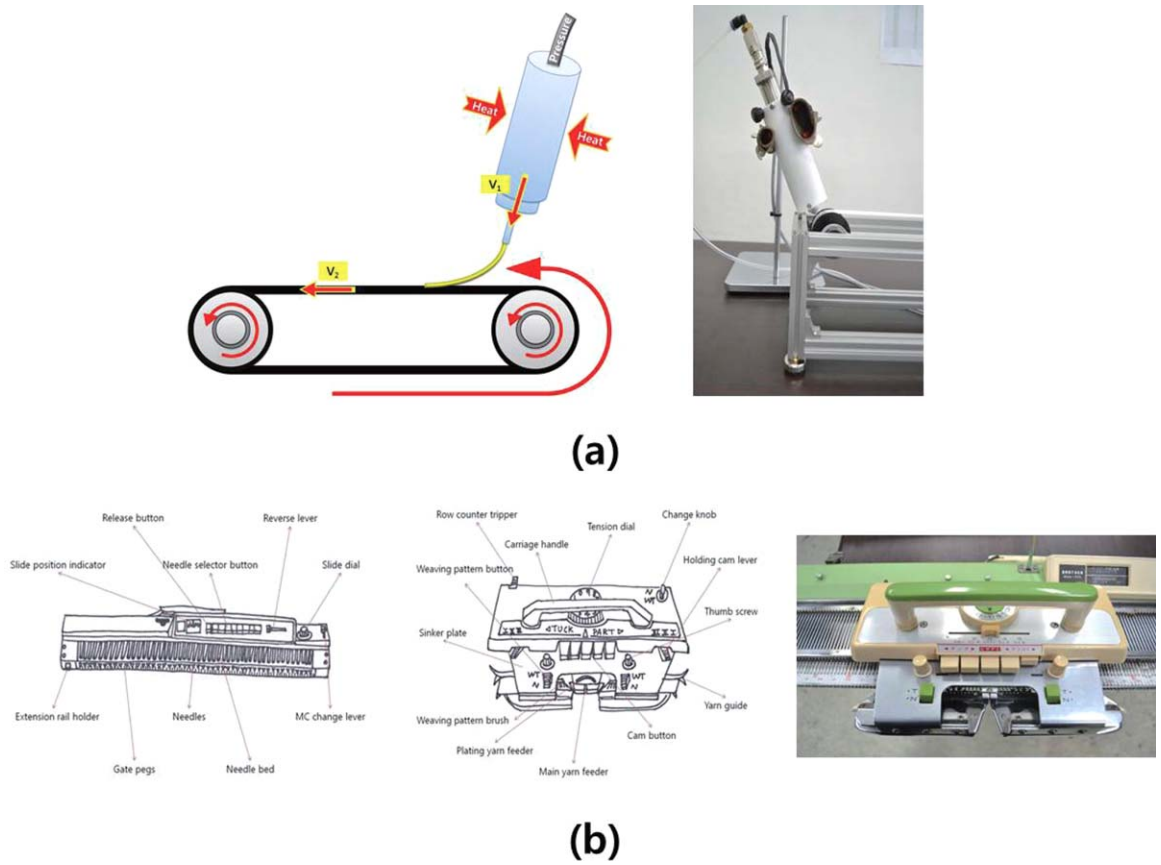


**Figure 1.** Schematics of (a) laboratory-made drawing machine and (b) knitting machine. [Color figure can be viewed in the online issue, which is available at wileyonlinelibrary.com.]

studies were performed to investigate the characteristics of knitting scaffolds.

In this study, various PCL knitting scaffolds were fabricated and analyzed to assess the cell-culturing characteristics of these scaffold with respect to pore-size heterogeneity, surface wettability, and surface roughness. First, six types of scaffolds were fabricated using chloroform and NaOH. The surface wettability and roughness of these scaffolds were measured to investigate the effect of chloroform and NaOH. Subsequently, the pore-size distribution of the fabricated scaffold was measured via microscopic investigation. Finally, the cell-culturing characteristics of these scaffolds were assessed via cell counting kit-8 (CCK-8), and Live/Dead assays on cells cultivated for 14 days.

## EXPERIMENTAL

### Materials

First, PCL (regent grade, $M_n = 70{,}000 \sim 90{,}000$, Sigma-Aldrich, St. Louis, MO) monofilaments having 150-μm-diameter were fabricated using extrusion and elongation process as shown in Figure 1(a). In extrusion process, heated (at 90°C) PCL was extruded with 1.26 mm/s speed [$V_1$ in Figure 1(a)] using dispenser nozzle of diameter 1.25 mm. In elongation process, the conveyor system moved at a speed of 88 mm/s [$V_2$ in Figure 1(a)] during extrusion process. Knitting was performed with a commercially available machine (KH-111, Brother, Japan) generally used in the hand-made clothing industry as depicted in Figure 1(b). Saos-2 cells were obtained from Korean cell line bank (KCLB).

### Fabrication of Scaffold

A control knitting scaffold was prepared using untreated PCL monofilaments 150-μm-diameter, as depicted in Figure 1(b) and Figure 2. A more detailed explanation of knitting process can be found in our previous study.[24] This type of scaffold was labeled "type C," where C indicates the control scaffold.

To fabricate another type of scaffold, we used process as depicted in Figure 2(b). Before the fabricated sheet was rolled up, chloroform was sprayed as shown in Figure 3(a). In this process, to fix the fabricated sheet and ensure all pores having similar size, stainless steel pins were stuck at the edge of the fabricated sheet on paper plate as depicted in Figure 3(a). Afterward, the paper plate was glued on the conveyor belt.

Chloroform was sprayed using an air-spray system (Infinity, Harder&Steenbeck, Germany) with a 0.2 mm nozzle, 0.2 MPa working pressure, and a 25 mm spraying distance. The conveyor system moved at a speed of 2.25 mm/s during spraying. After drying, the sprayed sheet was rolled up and diced to generate scaffolds. This type of scaffold was labeled "type RS," where RS means roughened sheet.

To fabricate a third type of scaffold, we used process as shown in Figure 2(a). Before fabricating the sheet, chloroform was

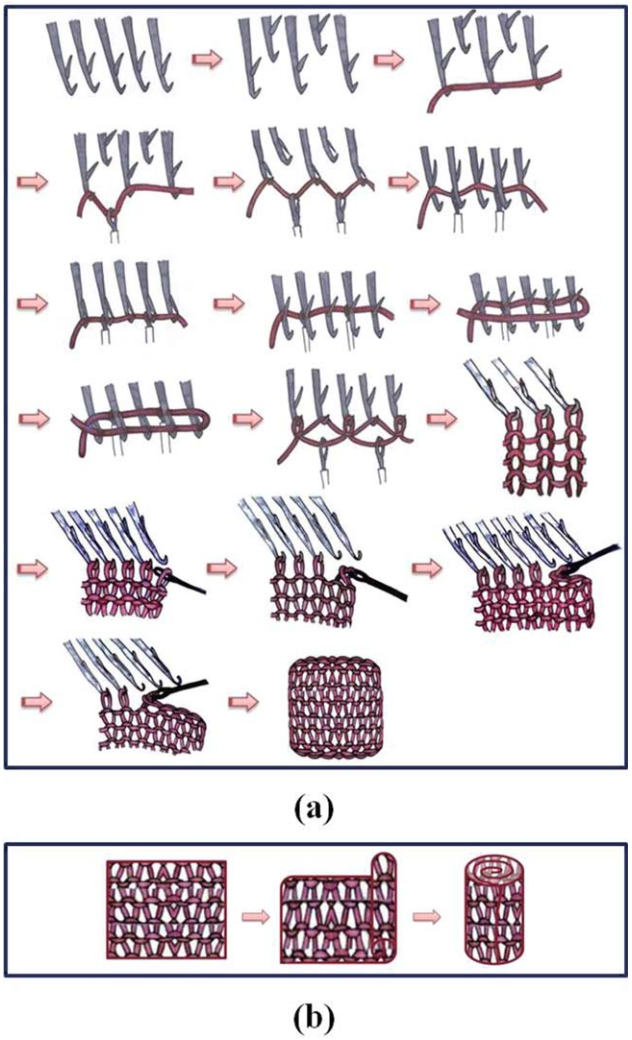


**Figure 2.** A schematic of the knitting scaffold fabrication process: (a) monofilament level and (b) sheet level processes. [Color figure can be viewed in the online issue, which is available at wileyonlinelibrary.com.]

sprayed as depicted in Figure 3(b). In this process, the prepared monofilament was moved at a speed of 2.25 mm/s, and chloroform was sprayed using an air-spray system (Infinity, Harder&-Steenbeck, Germany) with a 0.2 mm nozzle, 0.2 MPa working pressure, and a 25 mm spraying distance. After drying, sprayed monofilaments were used to fabricate the knitting scaffold. This type of scaffold was labeled "type RF," where RF means roughened filament.

To control the surface wettability of the scaffold or roughen the chloroform-treated scaffold surface, NaOH treatments were performed on the three types of scaffolds. The three types of scaffolds were soaked in 10*M* NaOH for 1 hour. After an hour, each scaffold was cleansed using deionized water.[28,29] These types of scaffolds were labeled "type C + NaOH,""type RS + NaOH," and "type RF + NaOH."

Table I provides descriptions of the abbreviations used for each scaffold type. Each scaffold was 5 mm in diameter and 5 mm in height. For each scaffold type, a total of 34 scaffolds were

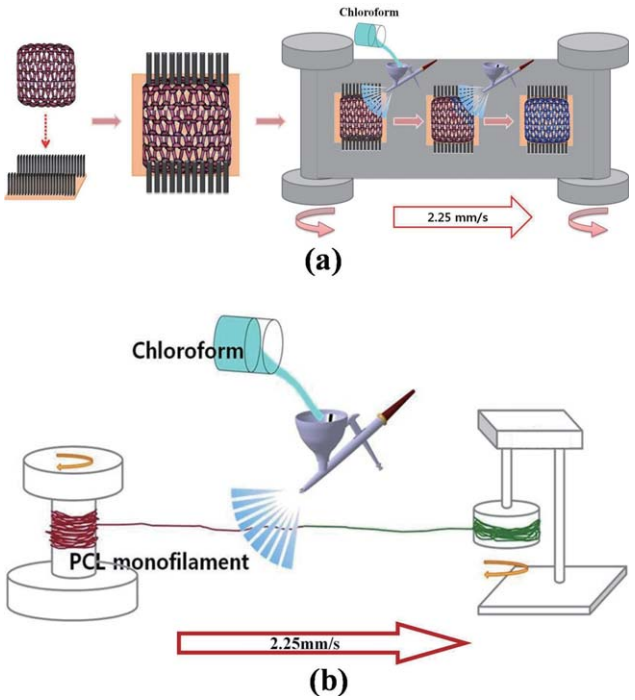


**Figure 3.** A schematic of (a) process used to fabricate RS type scaffolds and (b) process used to fabricate RF type scaffolds. [Color figure can be viewed in the online issue, which is available at wileyonlinelibrary.com.]

fabricated. For each type of scaffold, 20 scaffolds were used in the CCK-8 assay, 12 scaffolds were used in the Live/Dead assay, and 2 scaffolds were used for SEM images.

### Fabrication of Flat Sheets to Investigate Wettability, Roughness, and Chemical Changing

To investigate the influence of chloroform and NaOH on wettability and roughness, a PCL flat sheet was prepared. Surface wettability was measured using a contact anglemeter (SDL110TEZ, Femtofab Co.Ltd, Korea), and roughness was measured using a Scanning White Light Interferometer (NV 6300, Zygo).For this investigation, four different types of flat sheets(untreated PCL sheet, chloroform-treated PCL sheet, NaOH-treated PCL sheet, and chloroform/NaOH-treated PCL sheet) were prepared. The process conditions described above were used. A 5 μL water droplet was used for water contact

**Table I.** Explanation of Abbreviation of Scaffold Types

| Type of scaffold | Explanation of abbreviation |
|---|---|
| C | Control scaffold |
| RS | Chloroform-treated scaffold at the level of sheet[a] |
| RF | Chloroform-treated scaffold at the level of monofilament[a] |
| C+NaOH | NaOH-treated type C scaffold |
| RS+NaOH | NaOH-treated type RS scaffold |
| RF+NaOH | NaOH-treated type RF scaffold |

[a] Levels of sheet and monofilament were explanation detailed in Figure 1.

angle measurements, and three specimens of each type of flat sheet were used. Each specimen was measured three times. Three specimens of each type of flat sheet were also used for roughness measurements, and the average measured roughness is reported.

X-ray photoelectron spectroscopy (XPS) (Multilab2000, Thermo, UK) was performed to confirm chemical changes of surface on pure, NaOH-treated, and chloroform-treated PCL sheet scaffolds. The data of XPS spectra was generated and analyzed using the Avantage software.

**Characterization of Pore-Size Distribution, Porosity**

Optical microscope (Mi-9100 Zoom, Magiceyes, Korea) was used to approximately measure the pore-size distribution of fabricated scaffolds. The longest and vertical shortest distance from the longest one of 100 pores were measured for each type of fabricated scaffold, and pore-sizes were calculated using equation (1).[30,31,33]

$$\text{Pore size} = \frac{L_{\text{longest}} + L_{\text{shortest}}}{2} \quad (1)$$

where $L_{\text{longest}}$ is the longest length of randomly shaped pores and $L_{\text{shortest}}$ is shortest length of randomly shaped pores.

The porosity of fabricated scaffolds was calculated using equation (2). Twenty scaffolds were used to calculate the porosity of each scaffold type.

$$\text{Porosity} = \frac{v_0 - \frac{m}{\rho}}{v_0} \times 100\ (\%) \quad (2)$$

Where $v_0$ is the apparent volume of the scaffold, which is calculated using the outer dimension of the fabricated scaffolds; $m$ is the mass of the scaffold; and $\rho$ is the density of PCL.

**Cell Preparation and Live and Dead Assay**

After a few passages, cultured Saos-2 cells were detached using trypsin/ethylenediaminetetraacetic acid (EDTA) (0.05% w/v trypsin and 0.02% w/v EDTA) (Gibco BRL, Grand Island, NY). Scaffolds were sterilized with 70% ethyl alcohol overnight under UV light and were washed three times with phosphate-buffered saline (Hyclone). Saos-2 cells were seeded onto scaffolds at a concentration of $1 \times 10^5$ cells/10 μL in Dulbecco's Modified Eagle's Medium (DMEM; Hyclone, Utah) and incubated for 30 minutes to allow cells to attach to the scaffolds. After 30 minutes, medium was added, and cells were maintained in DMEM supplemented with 10% fetal bovine serum (FBS; Gibco BRL, Grand Island, NY), 100 U/mL penicillin (Gibco BRL, Grand Island, NY), and 100 μg/mL streptomycin (Gibco BRL, Grand Island, NY). The cell-culture was maintained at 37°C in a humidified incubator supplemented with 2% $CO_2$. To prevent the separating of cells from scaffold by suction process, half of the media was changed every 3 days.[32,33] Analytical assays were performed at 1, 3, 7 and 14 days.

To determine the seeding efficiency and cell growth on the scaffolds, viable cells were measured using Cell Counting Kit-8 (CCK-8, Dojindo, Japan) according to the manufacturer's instructions. Absorbance was measured at 450 nm using a micro plate reader every 30 minutes. Cell-proliferation data are presented as the mean optical density value from three walls and cell viability was assessed using a Live and dead assay kit (Molecular Probes) according to the manufacturer's instructions. Analytical assays were performed at 1, 3, 7 and 14 days. The scaffold was washed gently with PBS, and a solution of 2 μ*M* calcein AM and 4 μ*M* EthD1 was added. The scaffold was incubated at room temperature for 20–40 minutes. Calcein accumulates inside live cells with intact membranes, resulting in green fluorescent cells. This stain showed live attached to the scaffold.

**Statistical Analysis**

All data were presented as means ± standard deviation. Statistical analysis was conducted using single factor analyses of variance (ANOVA) through SPSS version 21.0 software program (SPSS, Chicago, IL). A value of $P < 0.05$ was considered statistically significant.

## RESULTS AND DISCUSSION

**Scaffold Morphologies via SEM**

Figure 4 shows SEM images of the six types of fabricated scaffolds at low magnification. Each SEM image was merged side to side using several SEM images. In the type C and C + NaOH scaffolds depicted in Figure 4(a,b), the surface of the monofilaments was very smooth compared to the type RF and RF + NaOH scaffolds, which are depicted in Figure 4(e,f). In the type RF and RF + NaOH scaffolds, which were treated with chloroform at the monofilament level, some roughened surfaces were detected. In addition, the type RS and RS + NaOH scaffolds depicted in Figure 4(c,d) exhibit molten shapes between the monofilaments. This morphology may be generated by spraying chloroform at the sheet level. In addition, to access influence for macroscopic morphology of fabricated scaffolds according to treatment of NaOH and chloroform, surface morphology of fabricated scaffold was observed at high magnification as shown in Figure 5. In all cases, there is no macroscale change was not detected comparing with the type C scaffold [Figure 5(a)].

**Water Contact Angle, Roughness, Porosity, and Chemical Changing with Respect to Treatment**

As mentioned previously, untreated PCL sheets, chloroform-treated PCL sheets, NaOH-treated PCL sheets, and chloroform/NaOH-treated PCL sheets were fabricated for wettability and roughness measurements. Although six types of scaffolds were tested (type C, RS, RF, C + NaOH, RS + NaOH, and RF + NaOH), from a chloroform and NaOH influence perspective, these scaffolds could be categorized into four types (untreated, chloroform-treated, NaOH-treated, and chloroform/NaOH-treated). Therefore, type RF and RS scaffolds may have similar characteristics to a chloroform-treated flat sheet. In addition, the type C + NaOH scaffold may have characteristics similar to a NaOH-treated flat sheet. Type RF + NaOH and RS + NaOH scaffolds may also be similar to the chloroform/NaOH-treated specimen.

As shown in Figure 6(a), the contact angle of water with the untreated PCL specimen was 69.4 ± 1.8°. After NaOH treatment, the water contact angle was reduced to 45.2 ± 4.7°. NaOH treatment[28,29] was commonly selected to fabricate

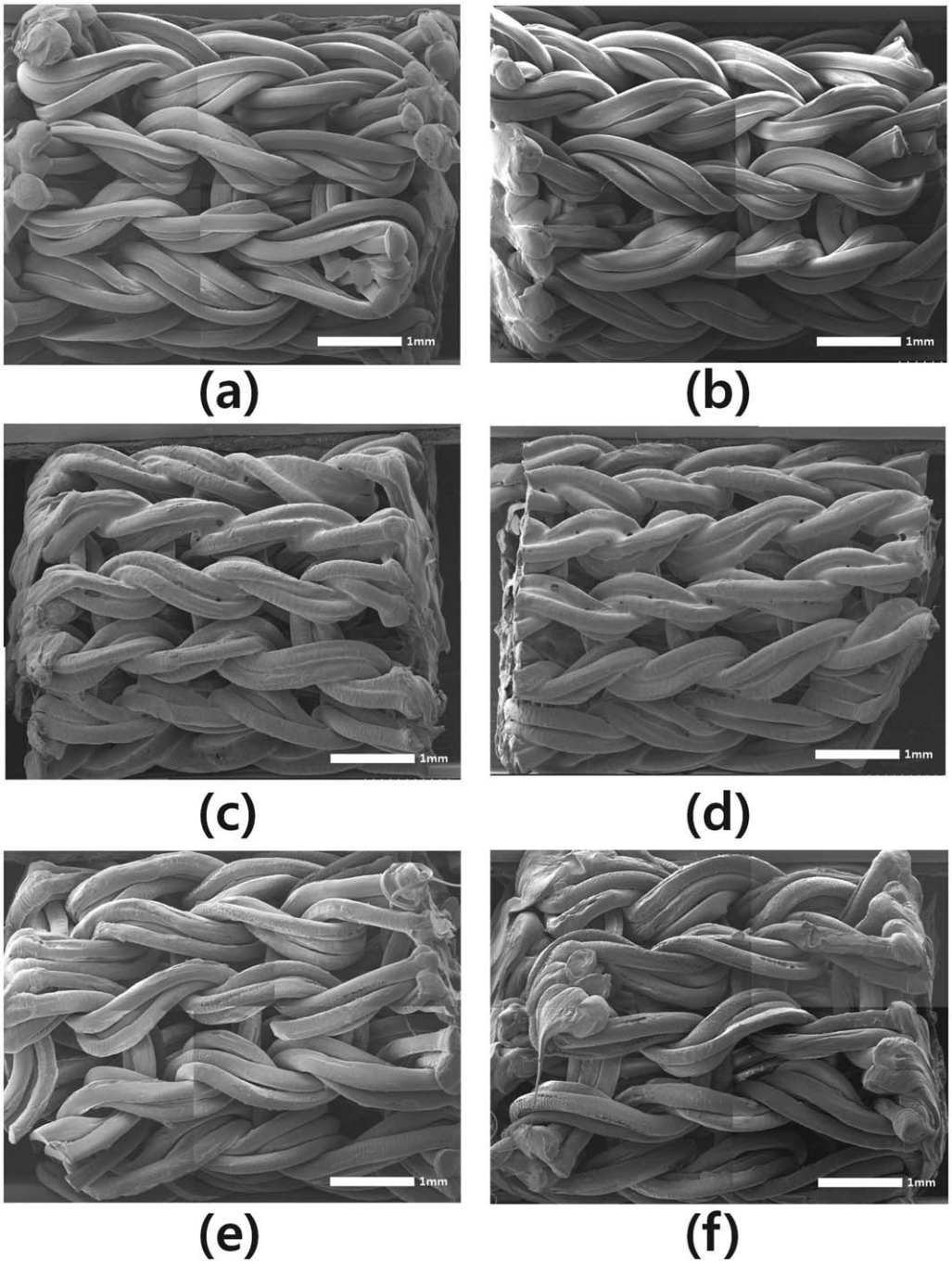


**Figure 4.** SEM images of fabricated scaffolds at low magnification(a) type C, (b) type C + NaOH, (c) type RS, (d) type RS + NaOH, (e) type RF, and (f) type RF + NaOH (scale bar: 1 mm).

hydrophilic PCL scaffold to enhance cell adhesion. NaOH treatment form —OH group on the PCL surface and the surface was changed as hydrophilic surface, because —OH group is hydrophilic. On the other hand, the water contact angle was increased to 115.3 ± 1.4° after chloroform treatment. After treatment with both chloroform and NaOH, the water contact angle was 117.1 ± 1.3°, similar to the contact angle for the chloroform specimen. A hydrophilic characteristic was expected for the chloroform/NaOH-treated specimen: because drying and cleaning were performed after treatment with chloroform, NaOH treatment of the chloroform-treated specimen was expected to produce a specimen with properties similar to the NaOH-treated bare PCL sheet. However, in our experiment, the water contact angle did not change when the chloroform-treated specimen was further treated with NaOH. Nevertheless, the roughness of the surface was increased, as shown in Figure 6(b).

As shown in Figure 6(b), the roughness value ($R_a$) of the untreated PCL specimen was 0.04 ± 0.01 μm. After NaOH treatment, the roughness value decreased slightly to 0.03 ± 0.01 μm.

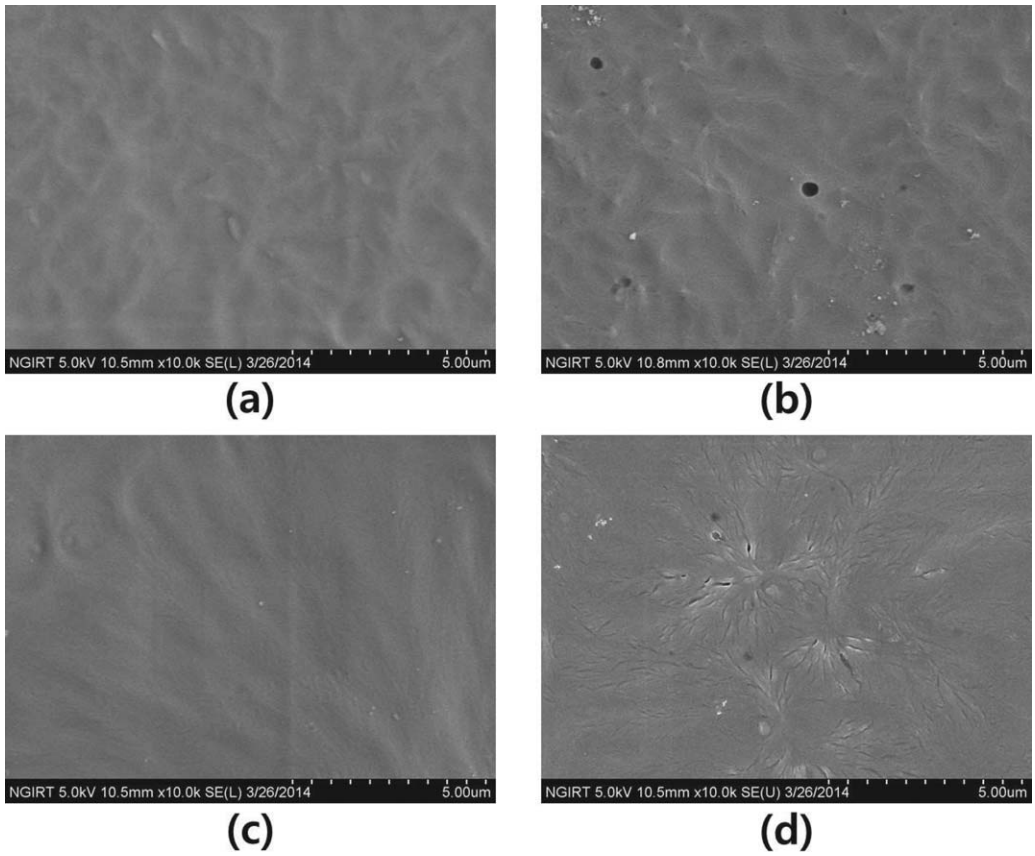


**Figure 5.** SEM images of fabricated scaffolds at high magnification (a) type C, (b) type C + NaOH (treated NaOH), (c) type RS and RF (treated Chloroform), (d) type RS + NaOH and RF + NaOH (treated Chloroform and NaOH) (scale bar: 5μm).

This change is not significant compared to the untreated specimen. However, after chloroform treatment, the roughness dramatically increased to $1.91 \pm 0.40$ μm. The roughness was further increased to $2.81 \pm 0.10$ μm after treatment with chloroform and NaOH. Commonly, in the viewpoint of surface engineering, it is obvious phenomenon that surface roughness increases the hydrophobicity of hydrophobic materials and the hydrophilicity of hydrophilic materials. To increase the surface roughness of PCL scaffold, chloroform was selected in this study, because chloroform is one of adequate solvents for PCL. Chloroform may dissolve PCL surface randomly and this process generates roughened PCL surface. For this reason, the roughness of chloroform-treated specimen was increased.

As depicted in Figure 6(C), the porosities of type C, RS, and RF scaffolds were measured. As mentioned previously, only type C, RS, and RF scaffolds were assessed, as it may be assumed that NaOH treatment does not result in any macroscopic morphology changes. Measured porosities were $49.4 \pm 0.5$, $47.1 \pm 0.4$, and $51.1 \pm 0.6\%$ for type C, RS, and RF scaffolds, respectively. Because all scaffolds had similar porosities, this parameter was assumed to not affect cell-culture characteristics of the scaffolds.

Figure 7(a,b) are XPS spectra of pure PCL, only chloroform-treated PCL, only NaOH-treated PCL, NaOH/chloroform-treated sheets. First of all, there is no detected peak related to Cl and Na. Therefore, residual chloroform and NaOH did not exist on specimens' surface. All detected peaks ($(CH_2)_n$, O═C—O, C—C, C—H, C—O, $(CH_3)_2$—C═O, C—H, and C═O) except C—OH and —OH in C1s and O1s spectra indicated the components of pure PCL.[34–36] C—OH and —OH peaks were generated by NaOH treatment and these group are hydrophilic.[37,38] For this reason, the wettability change of NaOH-treated specimen could be understood. However, in the case of chloroform/NaOH-treated specimen, $(CH_2)_n$ peak, which is hydrophobic, is more dominant compared to C—OH peak. Therefore, the hydrophobic characteristic of chloroform/NaOH-treated specimen could be explained.

### Pore-Size Distribution

In Figure 8, the pore-size distribution of each scaffold is depicted. Because it can be assumed that NaOH treatment does not result in any macroscopic morphology changes, only type C, RS, and RF scaffolds were assessed. As shown in Figures 8(a,c), there is no distinctive change in pore-size distribution of the type C and RF scaffolds. Furthermore, the pore-size distribution of the type C and RF scaffolds was very wide, ranging from 600 to 1100 μm. As shown in Figure 8(b), the pore-size distribution of the type RS scaffold was narrower than the type C and RF scaffolds. The pore-sizes of the type RS scaffolds were

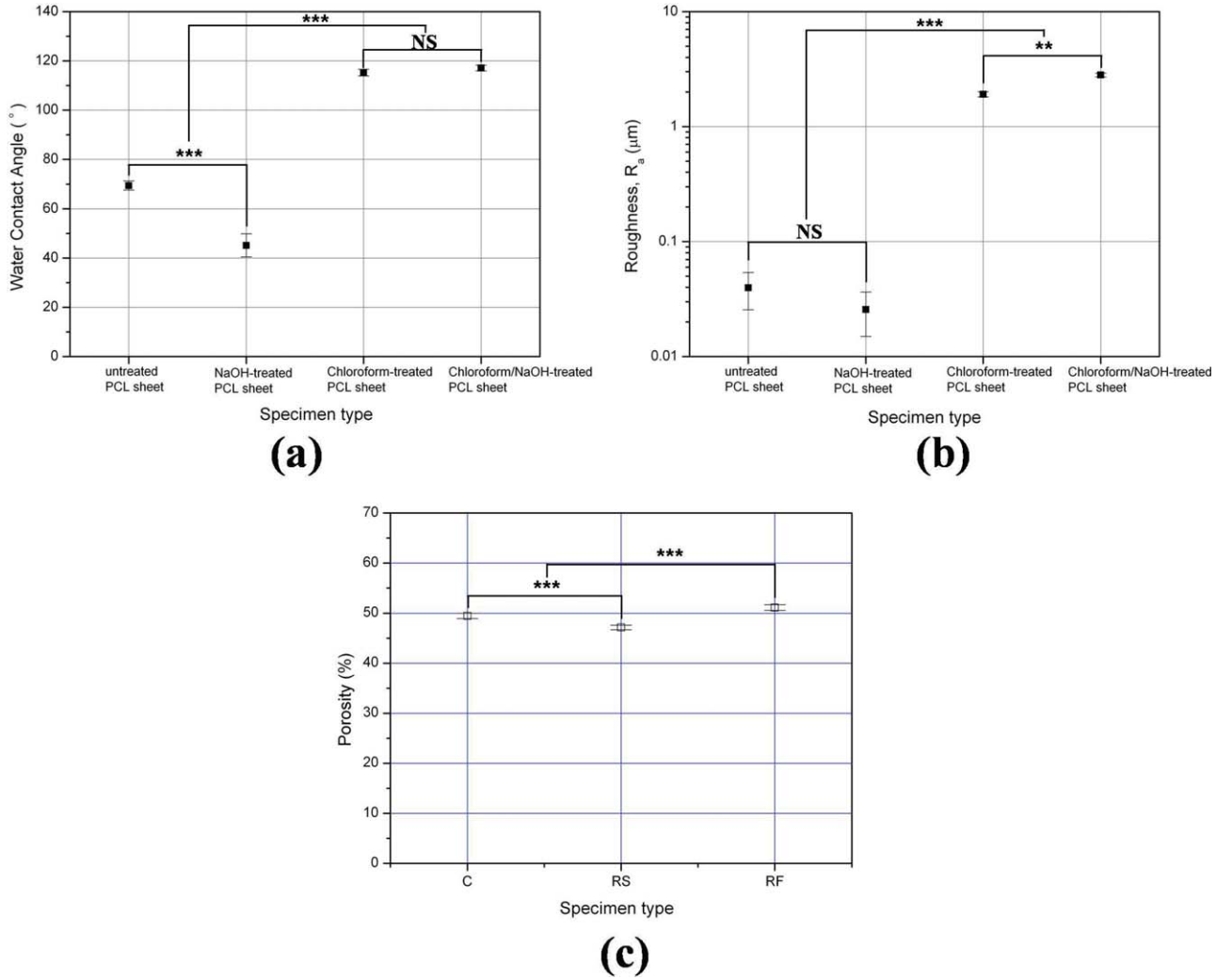


**Figure 6.** (a) water contact angles, (b) surface roughnesses, and (c) porosities with respect to types of scaffolds. [Color figure can be viewed in the online issue, which is available at wileyonlinelibrary.com.]

concentrated between 700 and 900 μm. Because RS scaffolds are fabricated via a process that fixes pore-sizes at the sheet level, final pore-sizes were concentrated within a narrower region compared to type C and RF scaffolds. However, it is too difficult to define the homogeneity of pore size. Therefore, in our study, the heterogeneity and homogeneity of pore size was divide qualitatively comparing to each other. Consequently, as depicted in Table II type RS and RS + NaOH were defined as "homogeneity" according to the result of Figure 8.

### Cell-Culturing Results

According to reported studies,[39–41] cell response of plotting scaffold with uniform pore size (homogeneous pore-size distribution) was better than that of salt-leaching scaffold with random pore size (heterogeneous pore-size distribution). However, plotting scaffold have well-interconnected pores and there are no interconnected pores in salt-leaching scaffold. Therefore, above-mentioned studies could be interpreted as a result of interconnectivity. However, in our study, we indicated that cell response of knitting scaffolds with heterogeneous pore size was better than that of knitting scaffolds with homogeneous pore size with same interconnected-pore condition.

In Table II, the pore-size distribution, wettability, and roughness for each scaffold type are outlined for easy understanding. Cell-proliferation results which are determined using CCK-8 assay are shown in Figures 9–11. To compare the effect of pore-size heterogeneity, RF vs. RS and RF + NaOH vs. RS + NaOH results are shown in Figures 9(a,b), respectively. To investigate the effect of wettability, C vs. C + NaOH results are shown in Figure 10. To investigate the effect of surface roughness, RF vs. RF + NaOH and RS vs. RS + NaOH results are shown in Figure 11(a,b), respectively. Type RF and RS scaffolds have different pore-size distributions but similar roughness and wettability as depicted in Table II.

As shown in Figure 9(a), the RF scaffold facilitated cell proliferation better than the RS scaffold, suggesting that pore-size heterogeneity is an important parameter for enhancing cell proliferation in knitting scaffolds. Figure 9(b), which compares the RF + NaOH and RS + NaOH scaffolds, provides further

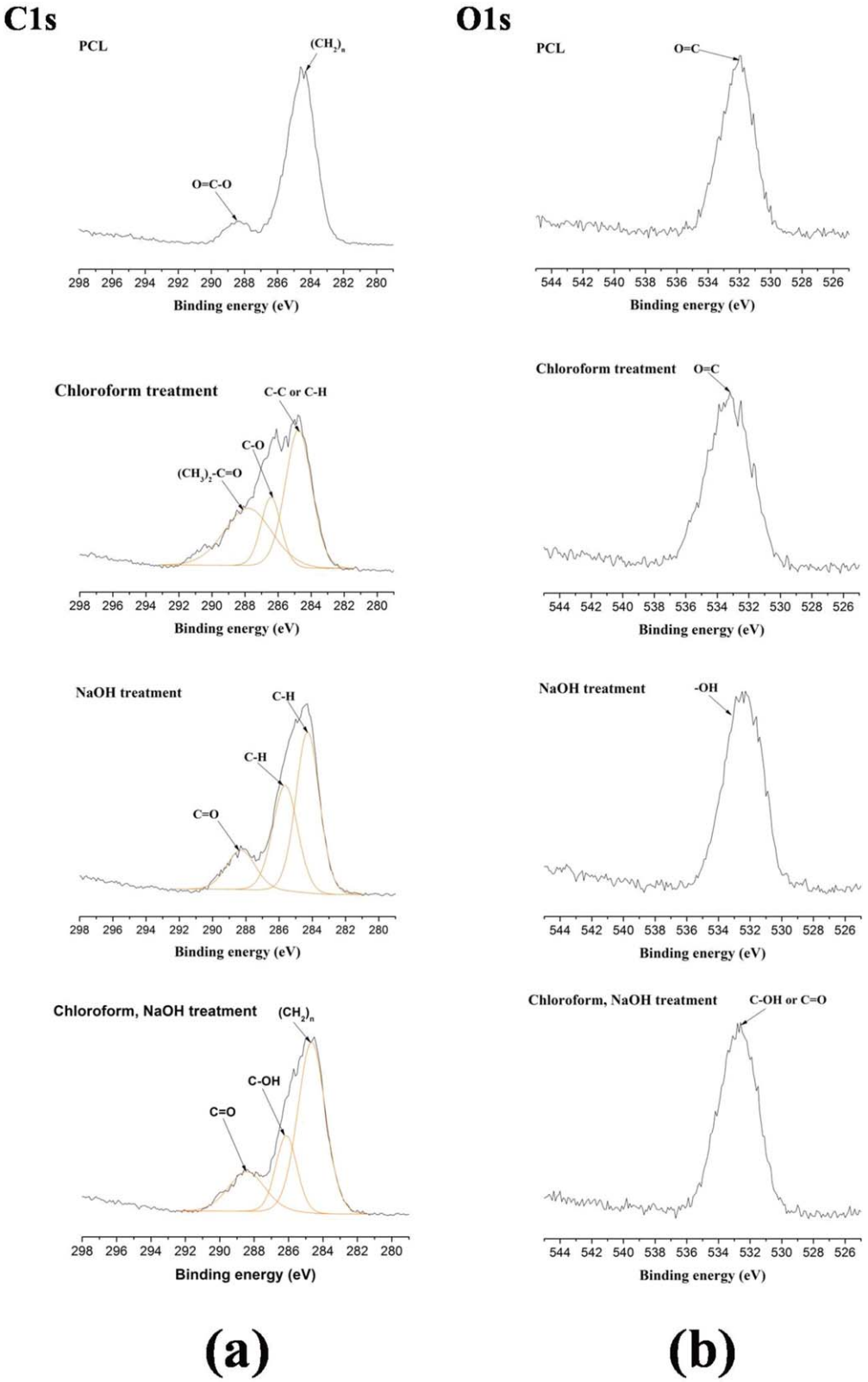


**Figure 7.** XPS spectra for pure PCL, chloroform-treated PCL, NaOH-treated, and NaOH/chloroform-treated PCL sheet: (a) C1s spectra and (b) O1s spectra. [Color figure can be viewed in the online issue, which is available at wileyonlinelibrary.com.]

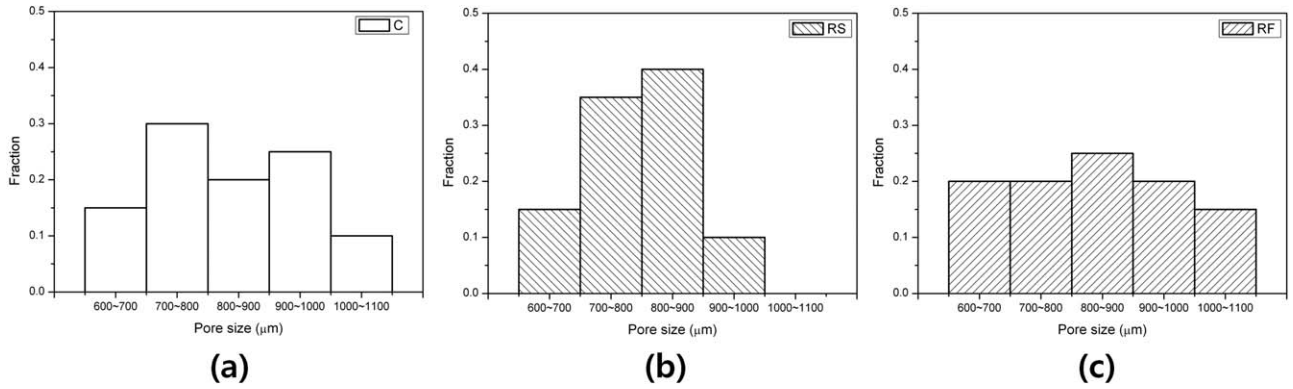


**Figure 8.** Pore-size distributions; (a) type C, (b) type RS, and (c) type RF scaffolds.

**Table II.** Pore-Size Heterogeneity, Surface Wettability, and Surface Roughness with Respect to Types of Scaffolds

| | | Wettabillity | | Roughness | |
|---|---|---|---|---|---|
| Type of scaffold | Pore-size heterogeneity (○: heterogenous, △: homogenous) | Water contact angle (CA, °) | ○: CA is under 50° ⊙: CA is under 80° ◉: CA is over 110° | Ra (μm) | □: Ra is under 0.1 μm ◘: Ra is under 2.0 μm ■: Ra is over 2.0 μm |
| C | ○ | 69.4 ± 1.8 | ⊙ | 0.04 ± 0.01 | □ |
| RS | △ | 115.3 ± 1.4 | ◉ | 1.91 ± 0.40 | ◘ |
| RF | ○ | 115.3 ± 1.4 | ◉ | 1.91 ± 0.40 | ◘ |
| C + NaOH | ○ | 45.2 ±4.7 | ○ | 0.03 ± 0.01 | □ |
| RS + NaOH | △ | 117.1 ± 1.3 | ◉ | 2.81 ± 0.10 | ■ |
| RF + NaOH | ○ | 117.1 ±1.3 | ◉ | 2.81 ± 0.10 | ■ |

evidence that pore-size heterogeneity enhances cell proliferation. Also, in the several previous studie,[33,42–45] there are some results to indicate that the pore-size distribution could affect the cell proliferation. Therefore, heterogeneity of pore size could be an important parameter for enhancing cell proliferation in the case of knitting scaffold.

Actually, RF + NaOH and RS + NaOH scaffold were initially expected that the water contact angle was low and the roughness was large comparing to the control scaffold. However, as a result, the water contact angle was not diminished after NaOH treatment. This issue should be studied for the further study. Anyway, as depicted in Figure 9(a,b), cell amount of RF and RS

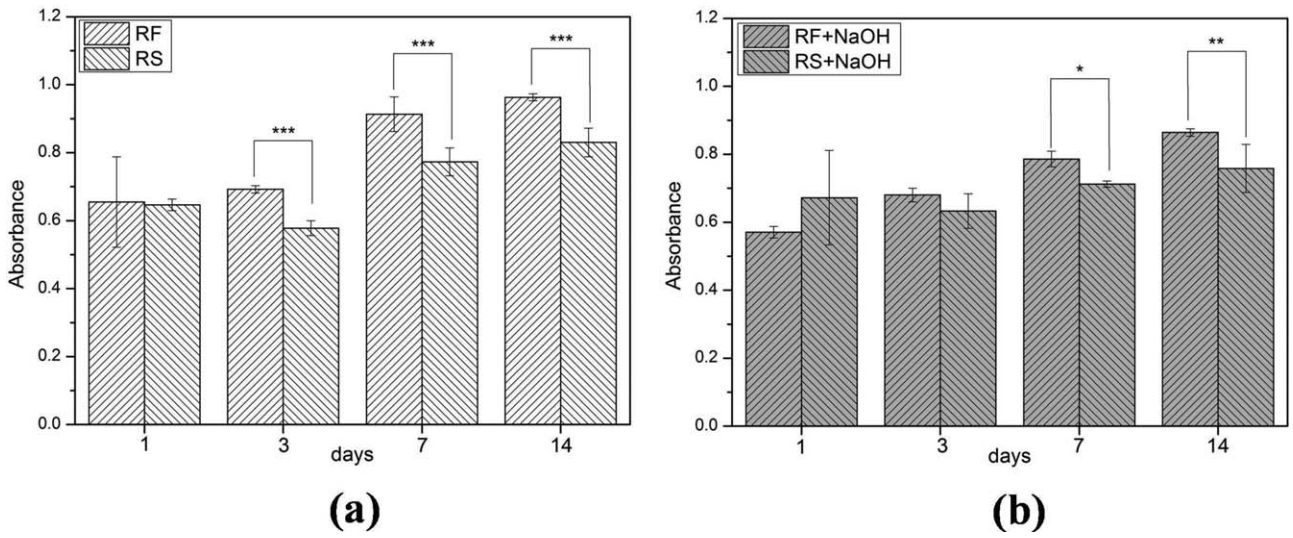


**Figure 9.** Cell-proliferation results with respect to pore-size heterogeneity: CCK-8 assay results of (a) RF vs. RS scaffolds and (b) RF + NaOH vs. RS + NaOH scaffolds.

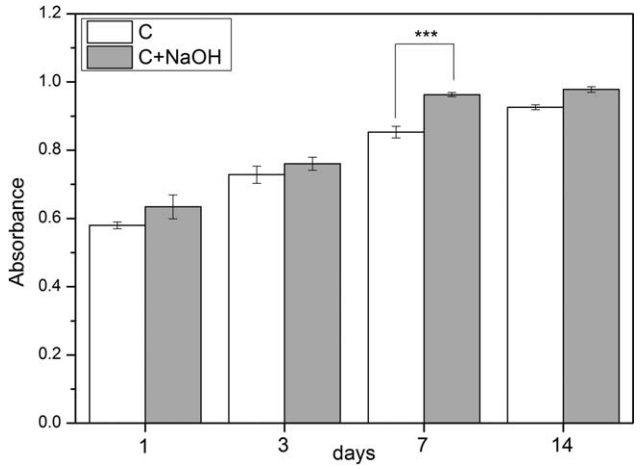


**Figure 10.** Cell-proliferation results with respect to wettability: CCK-8 assay results of C vs. C + NaOH scaffolds.

scaffold showed the inclination to decrease or maintain cell amount for 3 day comparing to 1 day. According to reported studies,[46,47] cell amount of pure PCL scaffold with hydrophobic characteristics for 3 days could be smaller than that of for 1 day. Moreover, in our previous study,[33] cell amount of pure PCL scaffold was decreased for 3 days comparing to cell amount for 1 day. This phenomenon could be understood as a result of hydrophobic characteristics of scaffold.

Figure 10 depicts cell proliferation measured using a CCK-8 assay on type C and C + NaOH scaffolds. Type C and C + NaOH scaffolds have different wettabilities but similar roughness and pore-size distribution. Figure 10 indicates that low wettability is important for cell proliferation in knitting scaffolds. Adequate wettability is known to be necessary for cell adhesion to the scaffold. In our work, enhancement of cell proliferation was observed after 7 and 14 days, as expected. According to the reported studies,[48–51] cell attachment/proliferation of the scaffold with hydrophilic characteristics was better than those of the scaffold with hydrophobic characteristics.

In Figure 11(a,b), cell proliferation measured via a CCK-8 assay of RF vs. RF + NaOH and RS vs. RS + NaOH are depicted. As mentioned previously, the chloroform/NaOH-treated scaffold has a similar water contact angle but different surface roughness compared to the chloroform-treated scaffold. Therefore, type RF and RF + NaOH scaffolds have different roughnesses but similar wettability and pore-size distribution. Type RS and RS + NaOH scaffolds also have different roughness but similar wettability and pore-size distribution. In our experiments, smaller roughnesses were better than larger roughness for the proliferation. However, this result is questionable, as the RF, RF + NaOH, RS, and RS + NaOH scaffolds were very hydrophobic. Hydrophobic scaffolds are not adequate cell scaffolds because cell attachment/proliferation of hydrophobic scaffold is unfavorable comparing to hydrophilic scaffold.[48–51] Therefore, these results must be carefully used to explain the effect of surface roughness. In the case of highly hydrophobic knitting scaffolds, increased roughness decreases cell proliferation.

In Figure 12, Live/Dead stain results were depicted at 1, 3, 7, and 14 days after cultivation of seeded cells for all types of scaffolds. It seemed that there is no bad influence of remained chloroform and NaOH according to Live/Dead stain results. Also, all types of scaffolds showed increasing cell-proliferation with respect to cultivation time.

## CONCLUSIONS

Knitting 3D scaffold was proposed and it was verified that the knitting scaffold is better than solid-freeform-fabricated scaffold in our previous study. As a follow-up study, the effects of pore-

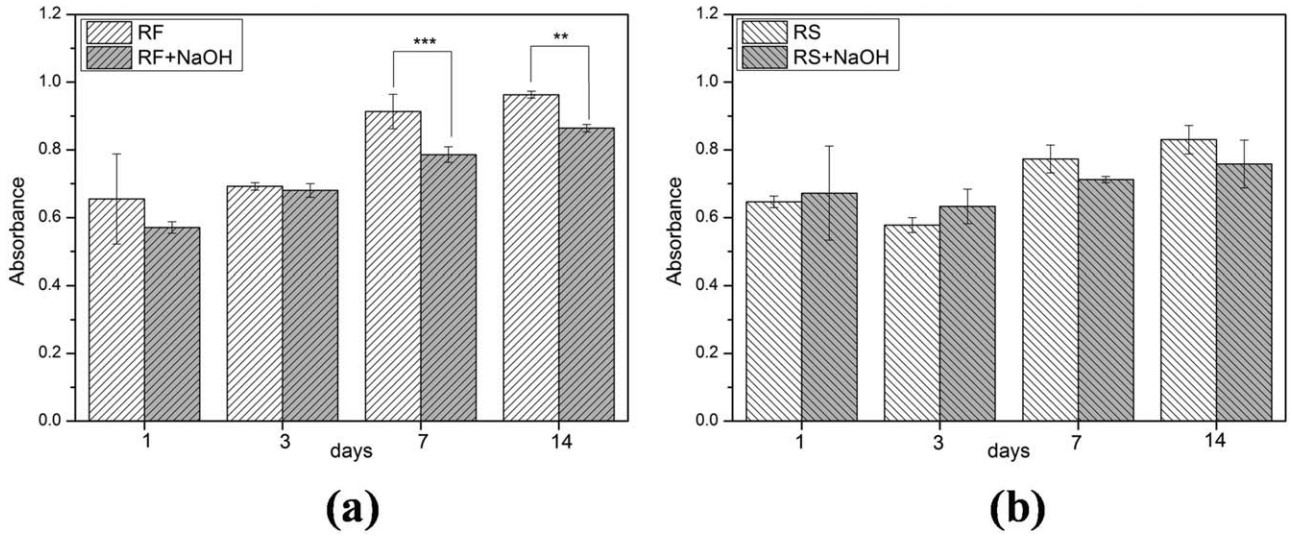


**Figure 11.** Cell-proliferation results with respect to surface roughness: CCK-8 assay results of (a) RF vs. RF + NaOH scaffolds and (b) RS vs. RS+NaOH scaffold.

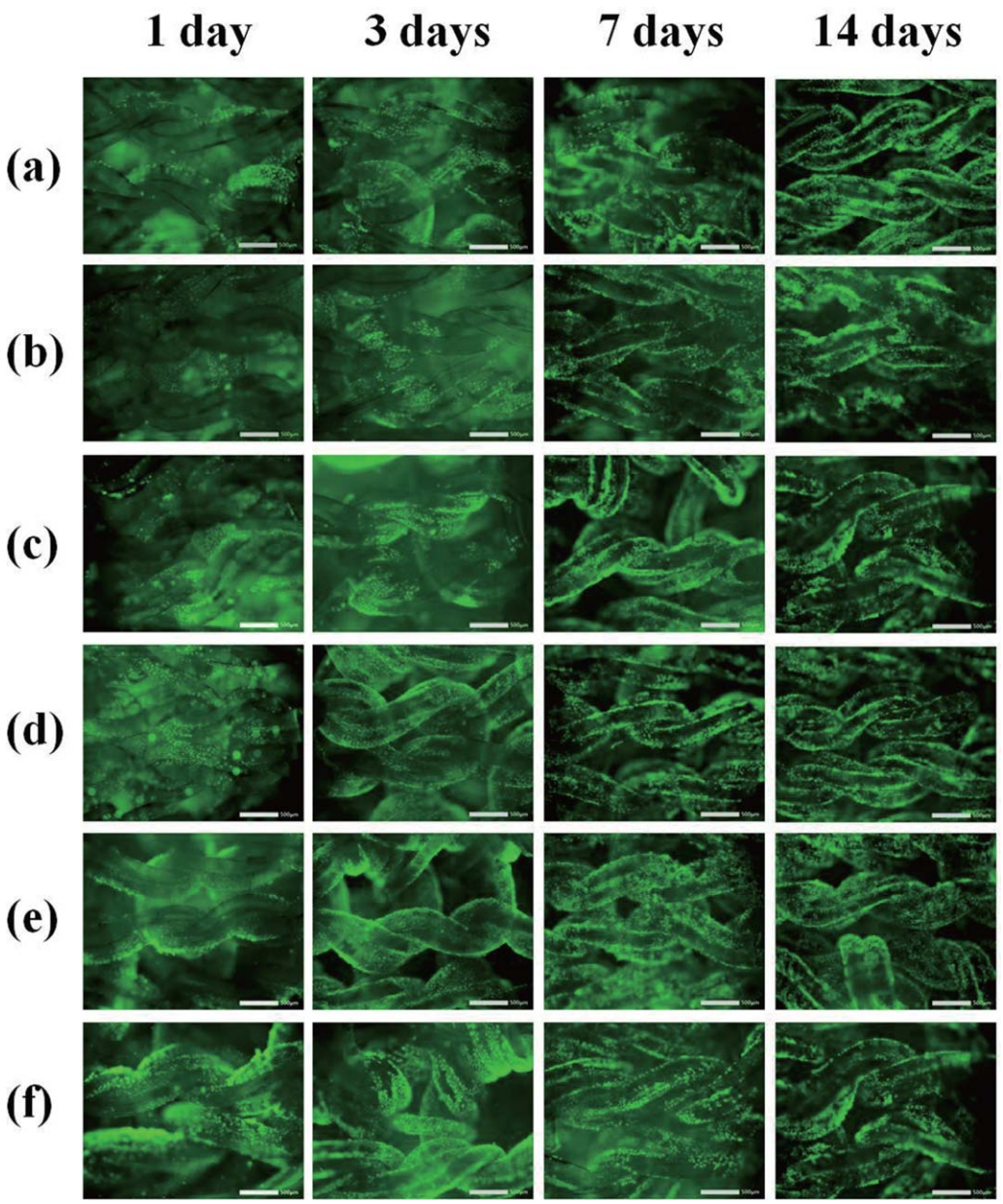


**Figure 12.** Observation of Live/Dead stain at 1, 3, 7, and 14 days after cultivation of seeded cells: (a) images of type C scaffold; (b) images of type RS scaffold; (c) images of type RF; (d) images of C + NaOH scaffold; (e) images of RS + NaOH scaffold; (f) images of RF + NaOH scaffold (scale bar = 500 μm). [Color figure can be viewed in the online issue, which is available at wileyonlinelibrary.com.]

size distribution, surface wettability, and surface roughness of knitting scaffolds were assessed in this study. Through NaOH treatment, —OH group was formed at the surface of scaffold. This surface modification made the scaffold hydrophilic. Also, chloroform treatment generated roughened surface at scaffold. It is confirmed that there is no residual NaOH and chloroform via XPS result. After this treating process, using Saos-2 cell, cell-culturing assessments were performed. Via cell-culturing assessments, pore-size heterogeneity, surface wettability, and surface roughness effects of 3D knitting scaffold was analyzed. Consequently, heterogeneous pore-size distribution and high surface wettability were found to enhance cell proliferation in knitting scaffolds. In addition, for highly hydrophobic knitting scaffolds exhibiting water contact angles greater than 110 degrees, smaller surface roughness was found to enhance cell proliferation. Because knitting scaffold have only been recently proposed, no parametric studies have been performed to understand the characteristics of knitting scaffolds. Therefore, although these results are quite restrictive, this work serves as a preliminary study that enhances our understanding of the characteristics of knitting scaffolds. According to this study, in the case of knitting scaffold, NaOH-treated knitting scaffold, without any control for the pore-size homogenization, could be a candidate as the optimal knitting scaffold. However, there still exist several issues to

be investigated to clarify the parameters for better cell proliferation in knitting scaffold.

## ACKNOWLEDGMENTS

This research was supported by Basic Science Research Program through the National Research Foundation of Korea (NRF) funded by the Ministry of Science, ICT & Future Planning (2014R1A1A1007298) and by a grant of the Korea Health Technology R&D Project through the Korea Health Industry Development Institute (KHIDI), funded by the Ministry of Health & Welfare, Republic of Korea (grant number: HI14C2143)

## REFERENCES

1. Sachlos, E.; Czemyszka, J. T. *Eur. Cells Mater.* **2003**, *5*, 29.
2. Hollister, S. J.; Maddox, R. D.; Taboas, J. M. *Biomaterials* **2002**, *23*, 4095.
3. Liu, X.; Ma, P. X. *Ann. Biomed. Eng.* **2004**, *32*, 477.
4. Hutmacher, D. W. *Biomaterials* **2000**, *21*, 2529.
5. Dehghani, F.; Annabi, A. *Curr. Opin. Biotechnol.* **2011**, *22*, 661.
6. Ahn, G.; Park, J. H.; kang, T.; Lee, J. W.; Kang, H. W.; Cho, D. W. *J. Biomech. Eng.* **2010**, *132*, 104506.
7. Cho, Y. S.; Hong, M. W.; Kim, Y. Y.; Cho, Y. S. *J. Appl. Polym. Sci.* **2014**, *131*, 40240.
8. Murphy, C. M.; Haugh, M. G.; O'brien, F. J. *Biomaterials* **2010**, *31*, 461.
9. Yeo, M. G.; Lee, H.; Kim, G. H. *Biomacromolecules* **2011**, *12*, 502.
10. Park, S. A.; Lee, S. H.; Kim, W. D. *Bioproc. Biosyst. Eng.* **2011**, *34*, 505.
11. Taboas, J. M.; Maddox, R. D.; Krebsbach, P. H.; Hollister, S. J. *Biomaterials* **2003**, *24*, 181.
12. Nam, Y. S.; Yoon, J. J.; Park, T. G. *J. Biomed. Mater. Res.* **2000**, *53*, 1.
13. Luong, N. D.; Moon, I. S.; Nam, J. D. *Macromol. Mater. Eng.* **2009**, *294*, 699.
14. Uematsu, K.; Hattori, K.; Ishimoto, Y.; Yamauchi, J.; Habata, T.; Takakura, Y.; Ohgushi, H.; Fukuchi, T.; Sato, M. *Biomaterials* **2005**, *26*, 4273.
15. Oh, S. H.; Kang, S. G.; Kim, E. S.; Cho, S. H.; Lee, J. H. *Biomaterials* **2003**, *24*, 4011.
16. Seyednejad, H.; Gawlitta, D.; Kuiper, R. V.; Bruin, A. D.; Nostrum, C. F. V.; Vermonden, T.; Dhert, W. J. A.; Hennink, W. E. *Biomaterials* **2012**, *33*, 4309.
17. Li, X.; Shi, J.; Dong, X.; Zhang, L.; Zeng, H. J. *Biomed. Mater. Res.* **2008**, *84A*, 84.
18. Chen, G.; Zhou, P.; Mei, N.; Chen, X.; Shao, Z. *J. Mater. Sci. Mater. Med.* **2004**, *15*, 671.
19. Jiankang, H.; Dichen, L.; Yaxiong, L.; Bo, Y.; Bingheng, L.; Qin, L. *Polymer* **2007**, *48*, 4578.
20. Jun, I. K.; Koh, Y. H.; Kim, H. E. *J. Am. Ceram. Soc.* **2006**, *89*, 391.
21. Malda, J.; Woodfield, T. B. F.; Vloodt, F. V. D.; Kooy, F. K.; Martens, D. E.; Tramper, J.; Blitterswijk, C. A. V.; Riesle, J. *Biomaterials* **2004**, *25*, 5773.
22. Marco, A.; Lopez, H.; Jerome, S.; Cedric, G.; Sophie, Q. *Biomaterials* **2008**, *29*, 2608.
23. Jo, A. R.; Hong, M. Y.; Lee, J. H.; Kim, Y. Y.; Cho, Y. S. *Tissue Eng. Regen. Med.* **2014**, *11*, 16.
24. Shor, L.; Güçeri, S.; Chang, R. *Biofabrication* **2009**, *1*, 015003.
25. Zein, I.; Hutmacher, D. W.; Tan, K. C. *Biomaterials* **2002**, *23*, 1169.
26. Hutmacher, D. W.; Schantz, T.; Zein, I. *J. Biomed. Mater. Res. A* **2001**, *55*, 204.
27. Kim, J. Y.; Cho, D. W. *Microelectron. Eng.* **2009**, *86*, 1447.
28. Sun, M.; Downes, S. *J. Mater. Sci. Mater. Med.* **2009**, *20*, 1181.
29. Zhou, Z.; Zhou, Y.; Chen, Y.; Nie, H.; Wang, Y.; Li, F.; Zheng, Y. *Appl. Surf. Sci.* **2011**, *258*, 1670.
30. Stokols, S.; Tuszynski, M. H. *Biomaterials* **2004**, *25*, 5839.
31. Mondrinos, M. J.; Dembzynski, R.; Lu, L.; Byrapogu, V. K. C.; Wootton, D. M.; Lelkes, P. I.; Zhou, J. *Biomaterials* **2006**, *27*, 4399.
32. Kim, S. E.; Rha, H. K.; Surendran, S.; Han, C. W.; Lee, S. C.; Choi, H. W.; Choi, Y. W.; Lee, K. H.; Rhie, J. W.; Ahn, S. T. *Macromol. Res.* **2006**, *14*, 565.
33. Cho, Y. S.; Hong, M. W.; Kim, S. Y.; Lee, S. J.; Lee, J. H.; Kim, Y. Y.; Cho, Y. S. *Mater. Sci. Eng. C* **2014**, *45*, 546.
34. Bichler, C. H.; Bischoff, M.; Langowski, H. C.; Moosheimer, U. 39th Annual Technical Conference of the Society of Vacuum Coaters, Philadelphia, USA, May 5, **1996**.
35. Wagner, C. D.; Riggs, W. M.; davis, L. E.; Moulder, J. F. Handbook of X-ray photoelectron spectroscopy; Muilenberg, G. E., Eds.; Perkin-Elmer Corporation, Physical Electronics Division: Minnesota, **1979**; Chapter 3, p 40.
36. Moncoffre, N.; Hollinger, G.; Jaffrezic, H.; Marest, G.; Tousset, J. *Nucl. Instrum. Meth. B* **1985**, *7*, 177.
37. Brown, N. M. D.; Hewitt, J. A.; Meenan, B. *J. Surf. Interface Anal.* **1992**, *18*, 187.
38. Briggs, D.; Seah, M. P. Practical Surface Analysis, 2nd ed.; Wiley: New York, **1993**; Vol. 2, Chapter 2, p 51.
39. Lee, J. W.; Kang, K. S.; Lee, S. H.; Kim, J. Y.; Lee, B. K.; Cho, D. W. *Biomaterials* **2011**, *32*, 744.
40. Lee, J. W.; Ahn, G. S.; Kim, J. Y.; Cho, D. W. *J. Mater. Sci: Mater. Med.* **2010**, *21*, 3195.
41. Lee, J. H.; Park, S. A.; Park, K. E.; Kim, J. H.; Kim, K. S.; Lee, J. H.; Kim, W. D. *Chinese Sci. Bull.* **2010**, *55*, 94.
42. Liang, W.; Rahaman, M. N.; Day, D. E.; Marion, N. W.; Riley, G. C.; Mao, J. J. *J. Non-Cryst. Solids* **2008**, *354*, 1690.
43. Malda, J.; Woodfield, T. B. F.; van der Vloodt, F.; Wilson, C.; Martens, D. E.; Tramper, J.; van Blitterwijk, C. A.; Riesle, J. *Biomaterials* **2005**, *26*, 63.

44. Hofmann, S.; Hagenmuller, H.; Koch, A. M.; Muller, R.; Novakovic, G. V.; Kaplan, D. L.; Merkle, H. P.; Meinel, L. *Biomaterials* **2007**, *28*, 1152.

45. Cho, Y. S.; Kim, B. S.; You, H. K.; Cho, Y. S. *Curr. Appl. Phys.* **2014**, *14*, 371.

46. Erisken, C.; Kalyon, D. M.; Wang, H. *Biomaterials* **2008**, *29*, 4065.

47. Tang, Y.; Zhao, Y.; Wong, C. S.; Wang, X.; Lin, T. *J. Biomed. Mater. Res A* **2013**, *101A*, 674.

48. Heo, S. J.; Kim, S. E.; Wei, J.; Hyun, Y. T.; Yun, H. S.; Kim, D. H.; Shin, J. W.; Shin, J. W. *J. Biomed. Mater. Res. A* **2009**, *89A*, 108.

49. Yeo, M. Y.; Lee, H. J.; Kim, G. H. *Biomacromolecules* **2011**, *12*, 502.

50. Yeo, M. G.; Kim, G. H. *Chem. Mater.* **2012**, *24*, 903.

51. Wei, J.; Yoshinari, M.; Takemoto, S.; Hattori, M.; Kawada, E. *J. Biomed. Mater. Res. B* **2007**, *81B*, 66.